We are IntechOpen,
the world's leading publisher of
Open Access books
Built by scientists, for scientists

6,900
Open access books available

186,000
International authors and editors

200M
Downloads

Our authors are among the

154
Countries delivered to

TOP 1%
most cited scientists

12.2%
Contributors from top 500 universities

CLARIVATE ANALYTICS
BOOK CITATION INDEX
INDEXED

WEB OF SCIENCE™

Selection of our books indexed in the Book Citation Index
in Web of Science™ Core Collection (BKCI)

Interested in publishing with us?
Contact book.department@intechopen.com

Numbers displayed above are based on latest data collected.
For more information visit www.intechopen.com

Chapter

Effect of Grain Size on Superplastic Deformation of Metallic Materials

Allavikutty Raja, Rengaswamy Jayaganthan, Abhishek Tiwari and Ch. Srinivasa Rakesh

Abstract

The superplastic deformation exhibited by metals with different grain sizes and their corresponding deformation mechanism influences the industrial metal-forming processes. The coarse-grained materials, which contain grain size greater than 20 µm, exhibited superplastic deformation at high homologous temperature and low strain rate of the order of 10^{-4} s^{-1}. Fine grain materials (1–20 µm) are generally considered as favorable for superplastic deformation. They possess high-strain-rate sensitivity "m" value, approximately, equal to 0.5 at the temperature of 0.5 times the melting point and at a strain rate of 10^{-3} to 10^{-4} s^{-1}. Ultrafine grains (100 nm to less than 1 µm) exhibit superplasticity at high strain rate as well as at low temperature when compared to fine grain materials. It is attributed to the fact that both temperature and strain rates are inversely proportional to the grain size in Arrhenius-type superplastic constitute equation. The superplastic phenomenon with nano-sized grains (10 nm to less than 100 nm) is quite different from their higher-scale counterparts. It exhibits high ductility with high strength. Materials with mixed grain size distribution (bimodal or layered) are found to exhibit superior superplasticity when compared to the homogeneous grain-sized material. The deformation mechanisms governing these superplastic deformations with different scale grain size microstructures are discussed in this chapter.

Keywords: grain size, superplasticity, deformation mechanism, coarse-grained superplasticity, fine-grained superplasticity, ultrafine-grained superplasticity, nano-grained superplasticity, superplasticity of mixed grain sizes

1. Introduction

Newtonian flow is the flow of a material in which the shear stress (τ) has linear relationship with the shear rate. The proportionality constant (μ) is called coefficient of viscosity. It is given by Eq. (1):

$$\tau = \mu \, \frac{dv}{dy} \tag{1}$$

The materials which exhibit Newtonian flow completely undergo shear by diffusion without the contribution of dislocations and cavities. If the relationship

between shear stress and shear strain is nonlinear, it is called non-Newtonian flow. Superplastic deformation is such a flow in which shear stress does not follow linear relationship. Backofen and Avery [1] proposed a power-law relationship for super-plastic deformation which is given in Eq. (2):

$$\sigma = K\dot{\varepsilon}^m \tag{2}$$

where σ is the true stress, $\dot{\varepsilon}$ is the strain rate, n is the strain-hardening exponent, *m* is the strain-rate sensitivity, and K is material parameter. For Newtonian fluids, *m* = 1. Superplasticity is exhibited by certain polycrystalline materials at the defor-mation temperature of above $0.5T_m$, where T_m is the absolute melting point of the material and strain rate ranges from 10^{-5} to 10^{-3} s^{-1} [2]. For a material to exhibit superplasticity, it should have stable, equiaxed, fine grain microstructure. Materials deformed at lower temperatures resist necking by work hardening, while superplas-tic materials resist necking due to the sensitivity of flow stress to strain rate, called strain-rate sensitivity (*m*) [3].

The superplastic materials generally exhibit m value greater than 0.3. Observations through scratch offsets at grain boundaries established grain bound-ary sliding (GBS) as a primary deformation mechanism [4–6]. Other than diffu-sional creep, dislocation creep and grain boundary sliding (GBS) were the different mechanisms that govern high-temperature deformation. Mukerjee et al. proposed a semiempirical relationship correlating strain rate, grain size, temperature, activa-tion energy, and stress to define the nature of superplastic deformation. The empiri-cal relationship is given by Eq. (3):

$$\dot{\varepsilon} = \frac{A D_0 G b}{kT} \left(\frac{b}{d}\right)^p \left(\frac{\sigma}{G}\right)^n \exp\left(\frac{-Q}{RT}\right) \tag{3}$$

where D_0 is the diffusion coefficient, G is the shear modulus, Q is the activation energy, T is the absolute temperature, R is the gas constant, b is the magnitude of the Burgers vector, d is the grain size, p is the grain size exponent, n is the stress
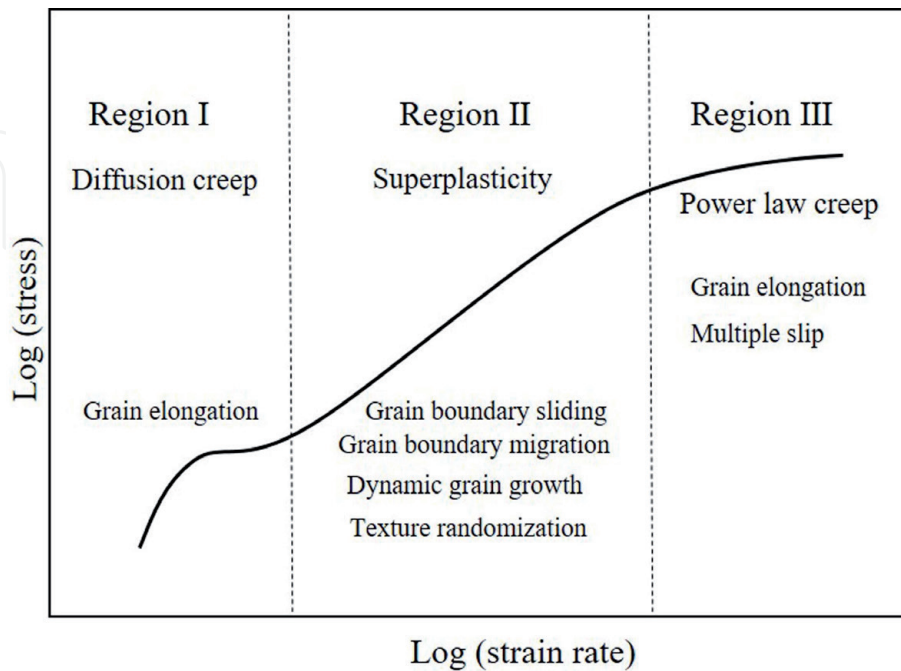

Figure 1.
Schematic illustration of the strain-rate dependence of flow stress in a superplastic material.

exponent (1/m), A is the constant dependent on microstructure and mechanism, and k is the Boltzmann constant. In general superplastic deformation was divided into three regions, as shown in **Figure 1**, based on the stress and strain rate range in which the deformation is taking place. The detailed discussion of these regions was discussed elsewhere [7]. The strain-rate dependence of stress, in turn, depends on the microstructure of the material and temperature range of the deformation. According to Eq. (3), the strain rate of superplastic deformation has an inverse relationship with grain size to the power "p." Moreover, with the advent of severe plastic deformation methods, fabrication of ultrafine grain (UFG) and nano-sized grains can be obtained using cryo forming [8, 9], multiaxial forging, equal-channel angular pressing (ECAP), friction stir processing (FSP), and high-pressure torsion (HPT). According to the Hall-Petch relationship, improvement in room-tempera-ture mechanical properties in different alloys was studied extensively [10–13]. The advancement in superplastic deformation due to these UFG and nano-grain sizes is multifold. They are high-strain-rate, low-temperature, and room-temperature superplasticity due to grain refinement and uniform thinning during superplastic bulge forming by controlling the grain size at the apex and edge. Hence, in this chapter, the effect of grain size varying from microscale to nanoscale on the super-plastic deformation was studied and discussed.

2. Superplastic deformation mechanisms

Three important deformation mechanisms at high-temperature deformation are diffusion creep, grain boundary sliding (GBS), and slip by dislocation move-ment. The mechanisms are common to both creep and superplasticity. Creep is the ability to resist deformation, while superplasticity is the ability to deform without necking. Diffusion creep is the vacancy movement. If the vacancy transfer occurs through grain boundaries, then the diffusion creep is called Coble creep. If the stress applied is parallel to grain boundaries, then the grain boundaries experience tension, while transverse grain boundaries experience compression (perpendicular to applied stress). As the vacancies occupy the transverse grain boundaries and get absorbed, a counter flux of atoms occurs toward the parallel-to-applied stress grain boundaries and causes grain elongation. If the vacancy transfers take place through the crystal lattice, then the diffusion creep is called Nabarro-Herring creep. Diffusion creep can be accommodated by another deformation mechanism GBS [4] and contains elongated grains [14]. The GBS that accommodates diffusion creep is called Lifshitz GBS. The other type of GBS called Rachinger GBS or simply GBS is a mechanism where adjacent grains are displaced at the grain boundaries between them but the grains remain equiaxed. GBS is impeded by obstacles like triple junctions or other types of stress concentration. Hence, GBS also required accommodation process. The accommodation process for GBS is delivered by slip activities like dislocation slip, grain rotation, grain boundary migration, and grain rearrangement [15, 16].

Dynamic recrystallization (DRX) is one another important deformation mecha-nism in many metals and alloys including Mg which produce fine grain micro-structure. Fine grain microstructure is essential to improve material's mechanical properties, and it helps in improving the superplastic elongation of the material. The important factors that influence DRX are initial grain size, second-phase par-ticles, stacking fault energy (SFE), thermomechanical processing, and severe plastic deformation conditions [17]. There are three types of DRX, namely, discontinuous DRX (DDRX), continuous DRX (CDRX), and geometric DRX (GDRX). Nucleation

of new grains and grain growth at the expense of regions full of dislocations are called DDRX [18] which is mostly observed during hot deformation of materials with low to medium SFE. In materials with high SFE, the subgrains or cell structure with low-angle grain boundaries (LAGBs) formed during deformation is gradually evolved into high-angle grain boundaries (HAGBs) due to efficient dynamic recovery, which is known as CDRX [19]. In material like aluminum, the grains elongate with local serrations at high temperatures and large strain. On further increase in strain, these serrations pinch off and form high-angle grain boundaries which are called GDRX [20].

3. Coarse-grained superplasticity

In 1982, Wadsworth et al. [21] fabricated a commercial C103 niobium alloy (Ni + 10 wt.% Hf + 1 wt.% Ti) by duplex hipping process for high-performance missile and space application systems. The microstructure of the fabricated metal had an average grain size of 75 μm. It exhibited a rupture at 125% elongation during a creep test at 1650°C. The deformation mechanism in this work was predicted as solute drag of dislocations caused by the diffusion of hafnium in niobium, which is of type class I solid solutions. Morgan and Hammond [22] used a method of pre-strain at high strain rate, region III of superplastic regime, followed by cyclic strain to generate subgrain boundaries inside the coarse-grained beta-Ti alloys. The material exhibited maximum elongation of 101% at 830°C. The superplastic deformation was due to diffusional creep mechanism. The vacancy generation and absorption were accommodated by the subgrain boundaries during the diffusional creep. In coarse-grained (62 μm) Ti40 alloy, the grains initially elongated and are then refined to lesser than 10 μm due to CDRA at 840°C and at a strain rate of 1×10^{-3} s^{-1}. It exhibited 436% elongation attributed lattice diffusion. Lin and Sun [23] reported 287.5% elongation in TiAl with 95 μm grain size at 1100°C and at a strain rate of 4×10^{-5} s^{-1} due to CDRX grain refinement followed by dislocation glide and climb accommodated GBS.

Woo et al. [24] observed superplasticity (300% elongation) in 150 μm grain-sized Al-Mg alloy due to diffusion of Mg in Al, solute-drag creep. Reduction in strain-rate sensitivity during solute-drag creep was observed in Al-Mg alloy after the addition of Mn or Zr. It is due to the change in the failure mechanism from necking-controlled-failure to cavitation-controlled-failure [25]. Further, Si addition on coarse-grained Al-Mg alloys also exhibited 350% elongation by solute-drag creep. Thus, Si addition, which did not affect the superplasticity but the high Si content of 0.2 wt%, formed higher volume fraction of Mg$_2$Si particles, which generates more cavity nucleation. These cavities reduce the post-forming tensile properties of the material [26]. On the addition Cu with Al-Mg alloy, the superplastic elongation (320%) was more than that of Al-Mg alloy (260% at 450°C and at a strain rate of 10^{-2} s^{-1}) [27]. Though the solute drag was explained as responsible deformation mechanism, the effect of Cu addition was not reported. When solute-drag creep was the responsible deformation mechanism, the material exhibited superplasticity at high homologous temperature as well as at high strain rate. Similarly, addition of Zn in Al-Mg alloy also improved the superplastic elongation due to solute drag coupled with CDRX before fracture [28]. Unlike GBS, solute-drag creep mechanism was independent of grain size. Hong [29] reported that if solid solution strength increases due to the increase in strain rate, during solute drag, it would increase the strain-rate sensitivity and superplastic deformation. Meanwhile, the microstructure would contain homogeneously distributed dislocations rather than dislocation clusters.

Malek [32] observed superplastic elongation of 150–200% in the coarse-grained Zn-1.1 wt.% Al alloy at 227°C and at a strain rate of 4.2×10^{-4} s^{-1}. The coarse-grained (70 µm) in this work was refined to fine grain size (20 µm) with straining due to CDRX. Similar results of CDRX was observed during superplastic deformation in the Fe$_3$Al-Ti alloy with 100 µm large grains when tested at 850°C at a strain rate of 1×10^{-3} s^{-1} [33]. Chu et al. [34] also observed superplastic elongation of up to 180% in Fe-27Al alloy with an initial grain size of 700–800 µm. The grain size reduced to 100–200 µm with strain due to continuous grain boundary migration, also called CDRX. CDRX is accountable only for grain refinement, but these works did not report about the superplastic deformation mechanisms. Mohri et al. [35] observed CDRX during superplastic deformation of rolled AZ91 Mg alloy with an initial grain size of 39.5 µm. The grain size reduced to 9.1 µm at a true strain 0.6 due to CDRX. The CDRX in Mg alloy was not because of the effect of SFE but due to the easily activated non-basal slip systems at elevated temperature. After grain refinement, GBS was observed to contribute in 604% superplastic elongation at 300°C and at a strain rate of 1.5×10^{-3} s^{-1}. On the similar mechanism of grain refinement followed by GBS, elongation of 512% was obtained by Lin et al. [36] in 155 µm grain-sized Mg-Li alloy at 250°C and at a strain rate of 5×10^{-4} s^{-1}. Wu and Liu [37] observed 320% elongation in 300 µm large grain Az31 alloy at 500°C and at a strain rate of 1×10^{-3} s^{-1}. The coarse grains were refined to 25 µm at a true strain of 0.024. In this work, grain refinement was reported due to dislocation slip and climb, while lattice diffusion controls the superplastic deformation, as the test was performed at higher temperature.

The coarse-grained materials exhibit superplastic elongation from 100% to maximum of 600% by AZ91 Mg alloy. The superplastic deformation mechanisms reported in coarse-grained materials are two types. First is the solute-drag creep in solid solution alloys like Al-Mg alloy with elongated grains as shown in **Figure 2**. The second one is the dynamic recovery and/or dynamic recrystallization followed by grain boundary sliding as shown in **Figure 3**.
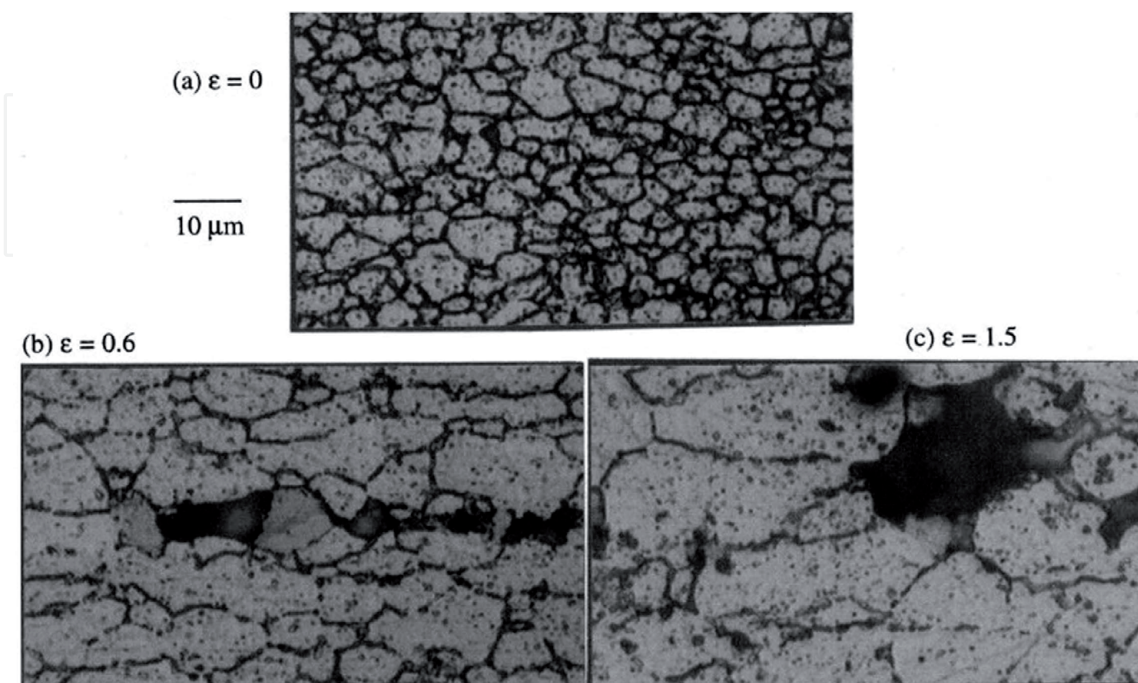

Figure 2.
Light optical micrographs of changes in the grain structure at a true strain of (a) zero, (b) 0.6, and (c) 1.5 at a tested strain rate of 5×10^{-4} s^{-1} [30].
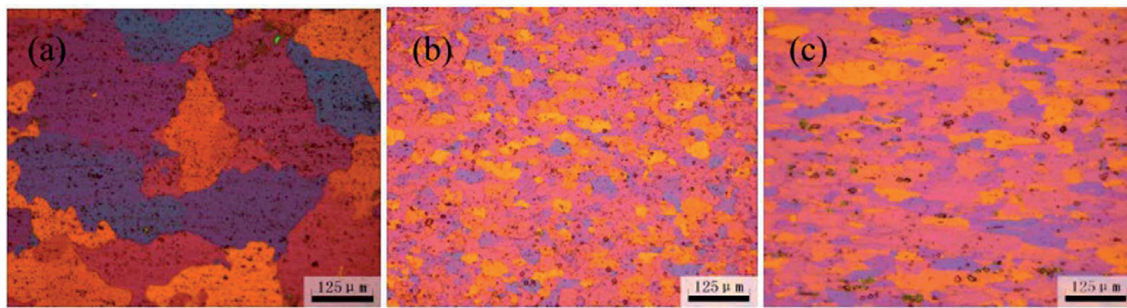
Figure 3.
Light optical micrographs of Al 5052 alloy deformed at 425°C and at a strain rate of 1×10^{-2} s^{-1} to (a) 10%, (b) 100%, and (c) 130% [31].

4. Fine-grained superplasticity

Fine-grained materials are generally preferred for superplastic deformation. Most of the materials deform by GBS; fine grains offer more fraction of grain boundaries when compared to coarse grains in a given area. As grain boundary slides, the moving dislocations need to be accommodated during the deformation process. Otherwise, dislocations would pile up at ledges or triple junction and generates stress concentration, eventually leads to cavitation and failure. Further, the slower accommodation mechanism if any or slower deformation mechanism which controls the superplastic deformation is termed as rate controlling mechanism. Hence, the deformation mechanism, accommodation mechanism, and rate-controlling mechanism are important in the fine-grained material. Zhou et al. [38] observed low-temperature superplasticity in 6 μm grain-sized Ti-6Al-4 V alloy at 700°C due to GBS accommodated by slip. However, the accommodation mechanism becomes grain boundary diffusion on increasing the temperature to 850°C.

In a work by Rao and Mukerjee [39] in fine-grained Al 7475 alloy, 840% elongation was attained during the tensile test at 457°C and at a strain rate of 1×10^{-4} s^{-1}. Grain elongation was observed with high dislocation density that leads to strain hardening in the material. Dislocation slip and climb through grains to the grain boundary was reported to cause grain elongation, together with grain boundary sliding. The measured activation energy, approximately 165 kJ/mol, was equal to self-diffusion of Al (142 kJ/mol). It describes that diffusion creep is the deformation mechanism rate controlled by dislocation climb. Mikhaylovskaya et al. [40] compared the superplastic deformation behavior in fine-grained Al 7475 alloy at primary stage and steady stage deformation. It was found that grain elongation occurred at primary stage due to diffusional creep, while at steady stage, diffusion creep becomes the accommodation process for GBS without any further change in the shape and size of the grain. Possibility of dislocation creep as an accommodation mechanism along with dislocation creep is also suggested in this work. This detailed study on the comparison between primary and steady stage deformation by Mikhaylovskaya et al. [40] elaborated and concurred with the work by Rao and Mukerjee [39].

In an interesting work by Fukuyo et al. [41], the accommodation mechanism for GBS in a fine-grained (6 μm) 10 wt.% Al-added ultrahigh carbon steel (UHCS-10Al) was studied. It was alluded that if stress exponent is equal to 2, then the accommodation mechanism was dislocation climb due to iron self-diffusion where if stress exponent reduced below 2, then dislocation glide due to solute drag is the accommodation mechanism. These values were confirmed by matching the measured Q values 191 kJ/mol and 292 kJ/mol with the theoretical Q values for self-diffusion (270 kJ/mol) and Al diffusion in Fe (155 kJ/mol), respectively.

In a fine-grained (2 µm) Mg-9Li alloy, the grain boundary diffusion accommodated GBS was reported as measured Q value of 67 kJ/mol was approximately equal to that of GBD (70 kJ/mol) [42]. This material exhibited superplastic elongation of 450% at 100°C. In a work by Kin and Chung [43], the deformation mechanism of 5 µm grain-sized AZ61 Mg alloy was reported to vary with the strain rate. At low strain rate, grain boundary diffusion-controlled GBS was deformation mechanism, whereas at high strain rates, pipe diffusion-controlled slip was the deformation mechanism. Maximum elongation of 560% was obtained at 400°C and at a low strain rate of 2×10^{-4} s^{-1}. As slip accommodates the GBS, slip systems in the direction of highest Schmidt factor has easier mobility which facilitates GBS accommodation. Anisotropy in superplastic elongation was observed in the fine-grained AZ61 alloy at 300–400°C by Wang and Huang [44]. However, the influence of Schmidt factors was limited to initial stages of deformation and below 400°C. At large strain, GBS and GBM would greatly reduce the texture effect, and above 400°C the difference in CRSS between different slip systems becomes negligible. GBS mechanism was compared in Al and Mg alloys by Wang and Huang [45]. The contribution of GBS was approximately 60% in Mg, while in the case of Al alloys, its contribution is around 20–30% at a true strain of below 0.5. It was because warm-extruded Mg alloy contains 88% HAGBs, while warm-worked Al alloy had 45–65% HAGBs. HAGBs favor GBS; hence, in Mg alloy almost every single grain contributes for GBS, whereas in Al alloys, the presence of LAGBs and CSL boundaries did not favor GBS. Hence, during initial stages of deformation, the group of grains with a common HAGB would undergo GBS, known as cooperative GBS. This initial strain promotes DRV/DRX to convert LAGBs into HAGBs and increase the fraction HAGBs at higher strain values. Further, in slip-accommodated GBS, slip process takes place by subsequent glide and climb. The distance of climb is an important factor in determining the strain rate. If the climb distance is of grain size, it would be absorbed by the grain boundary, and it would contribute for the elementary process of GBS. If the climb distance is of only core size of the grain, it would climb through the lattice and act as rate controlling process [46]. The superplasticity of AA 5083 alloy with and without Cr of grain sizes 7 and 10 µm was studied by Mikhaylovskaya et al. [47]. The elongation in alloy with Cr is found to be marginally higher than the alloy without Cr attributed to it difference in the grain size. It was found that contribution of GBS negligible in both these alloys, instead diffusion creep, was observed to be contributed for 50% of the strain rate. In particle-containing Mg alloys, which exhibit superplastic deformation at low temperature or room temperature, the GBS is accompanied by grain boundary migration. The cooperative effect of grain boundary sliding and migration creates stress concentration around the grains. The larger the GBS distance, the larger is the stress concentration, and depending on the grain orientation, migration aids in either stress relaxation or stress concentration [48]. This effect nucleates cracking of the particles inside the grain due to disclination; a rotational line defect arises out of rotational misfit between the lattices [49].

5. Ultrafine-grained superplasticity

Xu et al. [50] stated that superplastic deformation is one of the innovative applications of UFG alloys. Reducing the grain size aids in increasing the rate of superplastic deformation where GBS is the operative deformation mechanism. Kim et al. [51] proposed lattice diffusion-controlled GBS as a deformation mechanism for high-strain-rate superplasticity in 0.3–0.4-µm-sized grain Al alloy. Superplastic elongation of 9000% was achieved in an ultrafine-grained Ti-6Al-4 V alloy at 850°C [52]. However, Cu-Zn-Zr alloy exhibited superplasticity at a temperature

above 400°C and at strain rates below $1 \times 10^{-3} \text{ s}^{-1}$. It was because UFG was obtained by ECAP method which contains elongated grains. At temperature higher than the recrystallization temperature of the alloy, it exhibited superplasticity. Mere 0.18% addition of Zr helps in increasing the recrystallization temperature from 100 to 500°C that prevents grain growth. Zn inhibits dislocation creep and assists GBS in the process [53]. Ma et al. [54] achieved superplasticity in UFG Al alloy at a strain rate of 1 s^{-1} and at a temperature of 425°C due to lattice diffusion-controlled GBS.

Kawasaki and Langdon [56–58] developed deformation mechanism map for UFG polycrystalline materials depending on the strain rate and temperature range. Most of the materials, namely, Zn-22% Al and Pb-62% Sn alloys, fall in the range of region II of the superplasticity regime. Lee and Horita [59] observed low-temperature superplasticity in Al7075 alloy at 200–250°C due to UFG generated by high-pressure torsion process. In Al 5024 alloy, UFG grains of 0.7 μm was produced by ECAP and tested for superplasticity in the temperature range of 175–450°C and at a strain rate ranging from 10^{-3} s^{-1} to 10^{-1} s^{-1}. The material exhibited superplasticity in all the tested conditions due to grain boundary diffusion-controlled GBS. At 175°C the maximum elongation of 365% was obtained at a strain rate of $1.4 \times 10^{-4} \text{ s}^{-1}$, and at 450°C the maximum elongation of 3300% was obtained at a strain rate of $5.6 \times 10^{-1} \text{ s}^{-1}$. At low temperature, strain hardening was observed at the primary deformation stage due to the accumulation of lattice dislocations, whereas at high temperature, strain-induced grain elongation causes the strain hardening which accounted for the high-strain-rate superplasticity [55]. Bobruk et al. [60] demonstrated that UFG grain promoted low-temperature and high-strain-rate superplasticity in Al 7050 alloy. Edalati et al. [61] observed low-temperature superplasticity in Mg-Li alloy with 0.25 μm. The deformation mechanism was grain boundary sliding controlled by fast grain boundary diffusion due to Li segregation along the grain boundaries. The low-temperature superplasticity in this case was not attributed to UFG alone, but Li segregation in the boundary favors the grain boundary diffusion and GBS. Similar observation of maximum elongation of approximately 850% was found in UFG Ti-6Al-4 V (~0.4 μm) alloy due to high volume fraction of beta phase in a continuous network fashion acted as soft lubricant layer and increases the elongation [62]. Various deformation mechanisms that contribute for superplastic deformation in UFG regime were mapped with the optimum strain rate and temperature in **Figure 4**. It is evident that there
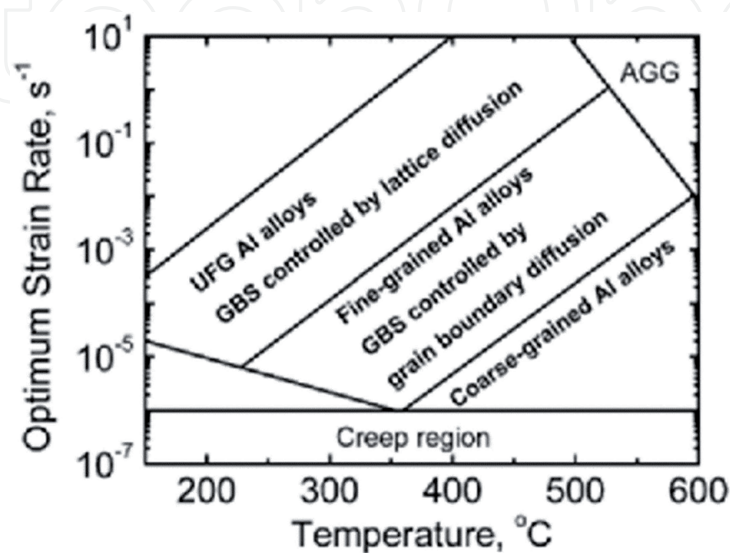

Figure 4.
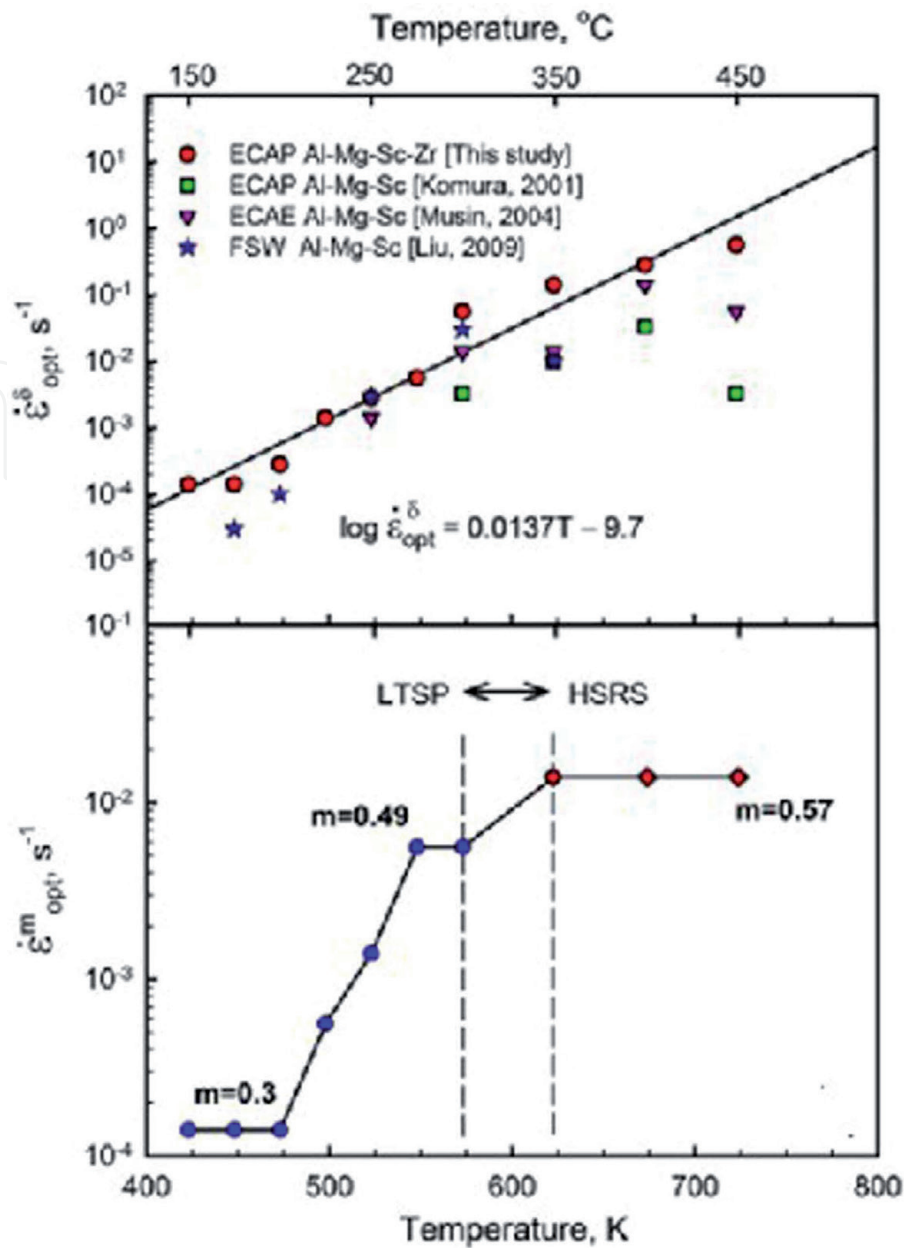*Superplastic mechanism map of FSP Al alloys [54].*

Figure 5.
Variation of optimum strain rate for maximum superplasticity (a) and optimum strain rate for the highest value of strain-rate sensitivity (b) with temperatures for ECAP Al-Mg-Sc-Zr and other UFG aluminum alloys [55].

is a relationship between temperature and strain rate. In **Figure 5**, an empirical relationship was presented with an illustration that HSRSP would take place at higher temperatures.

6. Nano-grained superplasticity

The kinetics of nano-grained superplasticity is different from the higher scale sized grains. Nano-grains show higher flow stress for superplastic deformation. It makes difficulty in activating the slip systems for the accommodation process [63]. The hypothesis for difficult slip accommodation is displayed in **Figure 6**. In the absence of slip as accommodation mechanism for GBS during nano-grained superplasticity, one of the possible accommodation mechanisms in nano-grains could be mobile triple junctions [64]. In nano-grained materials, partial dislocation slips can be activated at a lower stress level when compared to the perfect
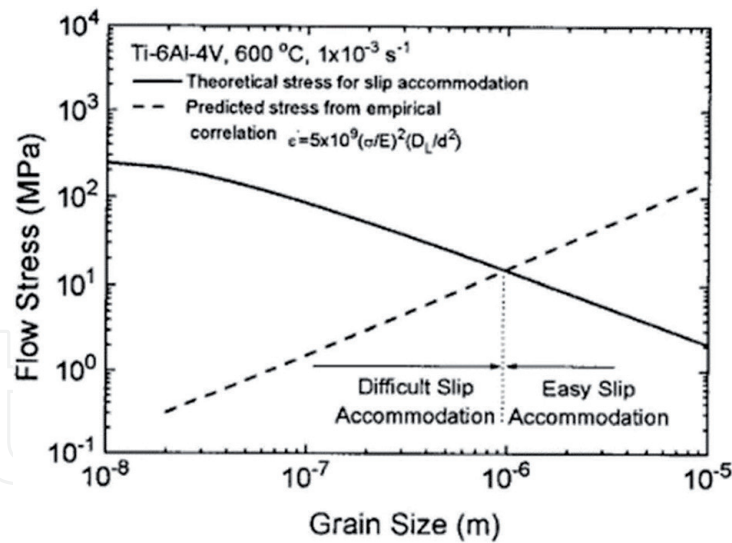
Figure 6.
A comparison of theoretical flow stress and empirical flow stress for slip accommodation in Ti-6Al-3.2Mo [63].

dislocation slips. As GBS occurs, dislocation accumulates at the triple junction which increases the system strain energy. The energy can be relaxed as Shockley partial dislocations emitted in to the neighboring grain. Thus, the emission of partial dislocations acts as an accommodation mechanism in nano-grained materials [65]. Similarly, dislocation transfer along a triple junction during grain boundary migration would increase the triple junction angle to accommodate the GBS [66]. Atomic shuffling accommodated GBS also suggested in nanomaterials [67]. The mechanism of atomic shuffling in tilt grain boundary during a shear is illustrated in **Figure** 7. This is called stress-induced grain boundary diffusion. In a defect-free single crystal, Au nano-wire superplastic deformation was found due to coherent twin propagation [68]. The test was carried in situ with SEM and HRTEM at room temperature, and the maximum elongation is only 50%, but the deformation mechanism reported in his work was interesting and specific to
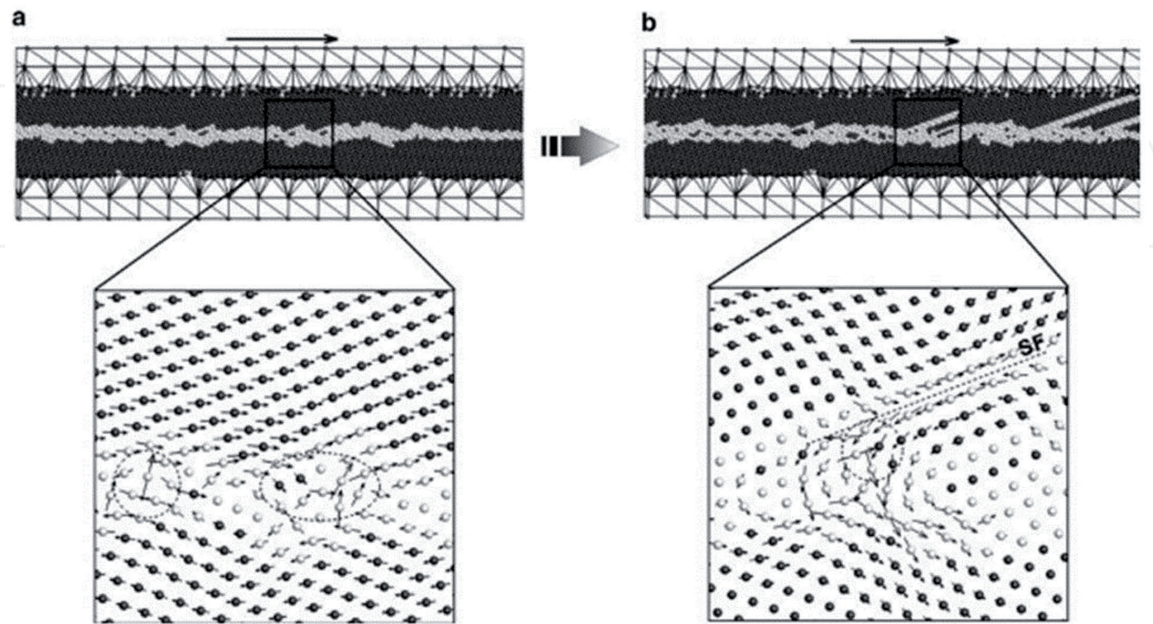

Figure 7.
Deformation mechanisms of a tilt GB under shear. (a) Early stage of GB sliding initiated by localized shuffling events (dashed circles) of atoms at the interface. Arrows correspond to the atomic displacement between two loading steps. (b) Subsequent stage of GB sliding where sites of atomic shuffling in the GB nucleate partial dislocations traveling into the grain and leaving a stacking fault (SF) [65].
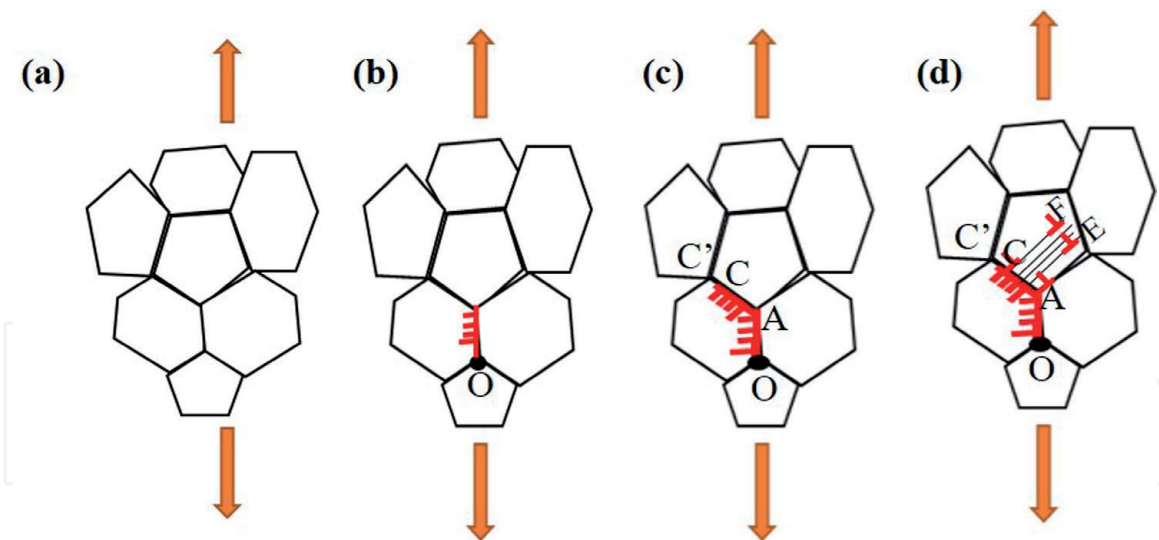
10

Figure 8.
Illustration of nano-twin formation during superplastic deformation. (a) Nanometer sized grains under tensile load, (b) GBS created dislocation pile up at triple junction O, (c) climb of dislocations on grain boundary AC', and (d) Nano-twin formation due to mobile partial dislocations that move into the adjacent grain interior, as grain boundary dislocations become sessile dislocations [69].

nano-grain superplasticity. The nano-twins observed to originate at the beginning of plastic deformation contain partial dislocations. Generally, the 1.54 GPa stress required to nucleate a partial in Au nano-wire, but due to nano-twins, the partials nucleated at the yield stress value of approximately 200 MPa. This nano-twin propagates by the glide of these partial dislocations. Ovid'ko and Skiba [69] figured out that the dislocation pile-up at the triple junction due to GBS caused nano-twin formation. The sequential step of GBS, dislocation pile-up, and twin formation are presented in **Figure 8**.

The piled-up dislocation splits in to two types: immobile GB dislocation and mobile partial dislocation. This partial dislocations then move cooperatively on every slip plane in a nanoscale region to generate nano-twin.

The evolution of nano-grains in to UFGs was observed in Al and Ti alloys which helps in improving the post-forming properties of the material [70]. Alizadeh et al. [71] reported grain boundary diffusion-controlled GBS in a nano-grained Mg-Gd-Y-Zr alloy when tested in the temperature range of 300–500°C. Similar to Li segregation at grain boundaries in UFG Mg-Li alloy, Edalati et al. [72] observed superplastic elongation at 300°C in nano-grained Al-Zn alloy due to the Zn segregation-enhanced GBS.

7. Superplasticity in materials with mixed grain sizes

Mansoor and Ghosh [73] studied the effect of multi-pass FSP on extruded ZK60 Mg plate. They found improvement in room-temperature mechanical properties of processed alloy, which was attributed to layered microstructure with grain size of 2–5 μm and 100 μm. Similarly, Witkin et al. [74] and Oskooie et al. [75] worked on Al alloys through cryo-milling and high-energy planetary ball-milling methods, respectively, to fabricate mixed-coarse and fine-grained structures and obtain optimum strength and ductility. Wang et al. [76] achieved enhanced strength and ductility in Cu after thermomechanical treatment with a mixed grain size distribution of micrometer-sized grains embedded inside a matrix of nano-crystalline and ultrafine (<300 nm) grains. The matrix grains impart high strength, whereas the coarse grains facilitate strain hardening mechanisms to give high tensile

ductility. Moreover, modifying the surfaces was reported to improve fracture and fatigue properties. Cáceres and Selling [77] mentioned that the area fraction of defects on the fracture surface influences the tensile properties rather than the bulk defect content. Begum et al. [78] found that that the fatigue cracks were originated from the surfaces with large grains. Perron et al. [79] performed molecular dynamic simulation on polycrystalline Al samples and found a linear relationship between grain size and surface roughness to an extent of applied strain, while Liu et al. [80] reported that surface modification by shot peening decreases surface roughness due to grain refinement and becomes the reason for improvement in mechanical properties in Mg alloy.

At high temperature, the effect of fine grains is substantial; even room-temperature superplasticity was observed after HPT in pure Mg [81] and in Mg-Li alloy [61]. However, few studies showed superplasticity in coarse-grained Mg alloys also. Watanabe et al. [82] achieved superplastic elongation of 196% in AZ31 Mg alloy with an average grain size of 130 μm. Wu and Liu [37] reported superplasticity of 320% in hot-rolled AZ31 Mg alloy with a mean grain size of 300 μm. Grain size was found to reduce to 25 μm during deformation due to dislocation slip and climb. Hence, the idea of mixed grain size microstructure which showed promising improvement in room-temperature mechanical properties was explored at high temperature also. Fan et al. [83] observed more superplastic elongation in AA8090 Al-Li alloy which inherently contains three distinct microstructural layers through the thickness when compared to superplasticity of surface layers (equiaxed grains) and middle layers (elongated grains) alone as shown in the **Figure 9**. Pancholi and Kashyap [84] obtained better bulge profile during superplastic bulge forming of AA8090 Al-Li alloy.
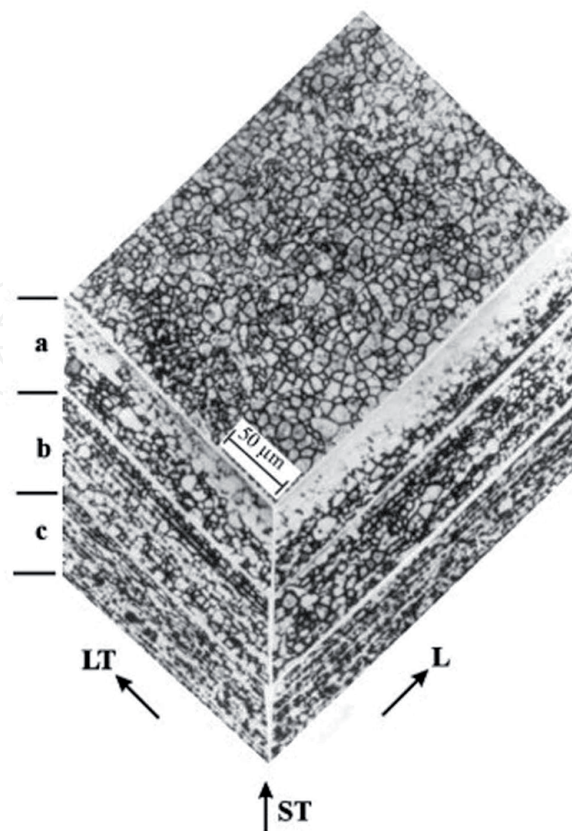

Figure 9.
Three-dimensional view of the microstructure after annealing at 540°C for 5 min: (a) Li-depleted layer, (b) layer with recrystallized microstructure, and (c) middle layer of un-recrystallized grains [84].

Later, Pradeep and Pancholi [85] deliberately fabricated layered microstructure containing coarse and fine grains in Al 5082 alloy using FSP and found that the inhomogeneous microstructures possess superior superplastic formability than the homogeneously grain-sized materials. It can be clearly observed in **Figure 10** that the composite layer (CL) contains the mixture of thermomechanically affected layer (TL) and nugget layer (NL) contains lesser fraction for cavities and maximum elongation as evident from its necking. Álvarez-Leal et al. [86] observed superplasticity in extruded ZK30 Mg alloy. During deformation the complex as received microstructure evolved into bimodal microstructure.

In general, inhomogeneity in initial material would lead to inhomogeneous deformation and strain localization which eventually lead to failure [89]. In classical superplastic literature, uniform fine-grained microstructure was considered favorable for superplasticity. However in Al alloys, inhomogeneous microstructure has shown to exhibit higher ductility than homogeneous fine-grained microstructure [74–76, 87]. Pancholi et al. [90] demonstrated that at least 50% fine grain microstructure is required in the Al 5086 alloy for it to exhibit superior superplasticity when compared to the homogeneous fine-grained material. It was argued that microstructural refinement in the remaining 50% of coarse-grained microstructure, which leads to fully homogenous microstructure in the material, was the reason for higher superplasticity [84, 87]. However in the work by Raja and Pancholi [88], layered microstructure material exhibited elongation lower than fully fine-grained microstructure. The coarse grain with as-cast material is deformed by twins as shown in **Figure 11(a)**. The nature twins were found out to be extension-type from the misorientation distribution in **Figure 11(b)**. Lack of superplasticity in half thickness fine-grained material (HFG) and surface modified by fine-grained material (SFG) can be attributed to insignificant microstructural refinement in the coarse-grained as-cast microstructure during deformation, as shown in **Figures 11(c)** and **9(d)**. It is well established that Al alloys exhibit continuous dynamic recrystallization (CDRX) [91, 92], whereas AZ91 Mg alloys exhibit discontinuous dynamic recrystallization [93]. It appears that CDRX of coarse grains in the layer microstructure of Al alloys was the primary reason for higher
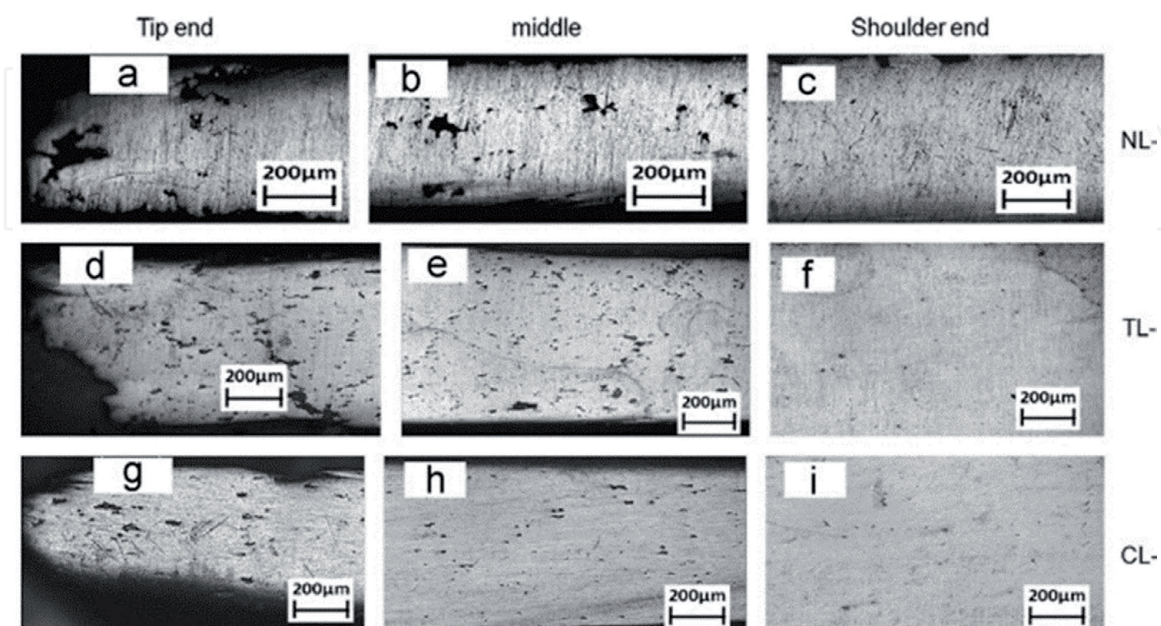

Figure 10.
Cavitation along the gauge length (in the thickness direction) at different points (tip end, mid-section, and shoulder end) of the tensile samples deformed at 500°C with a strain rate of $1 \times 10^{-3} s^{-1}$. (a–c) NL, (d–f) TL, and (g–i) CL [87].
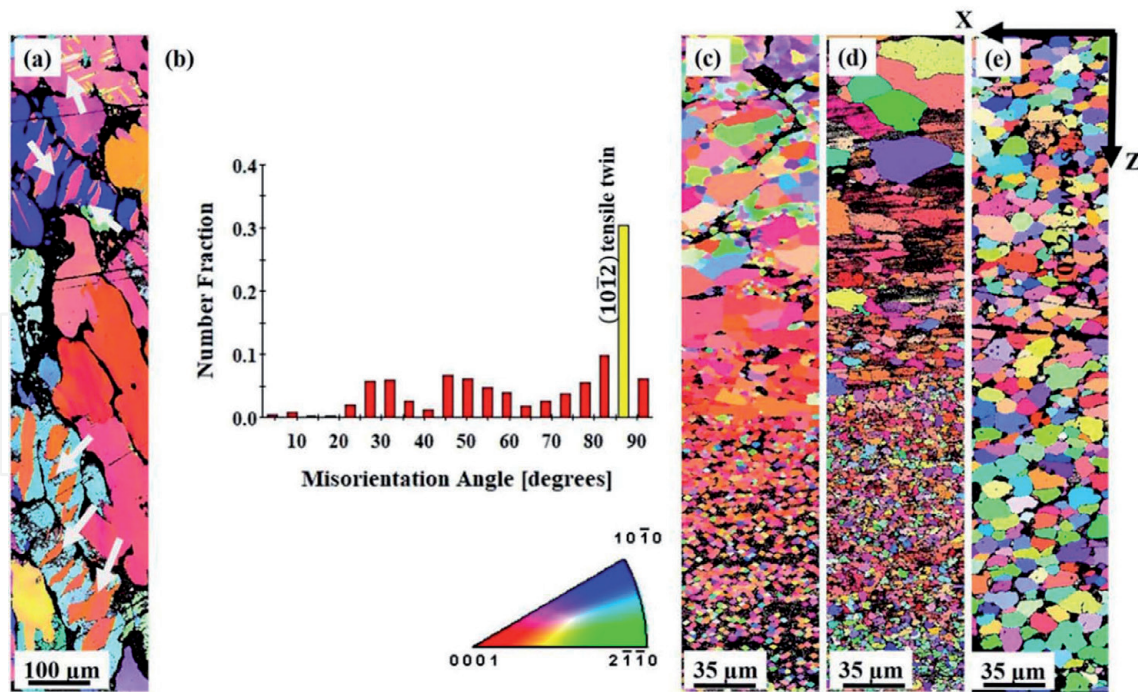
Figure 11.
IPF maps of deformed samples with tensile axis parallel to process direction (parallel to X-axis shown above) at a strain rate of $5 \times 10^{-4} \, s^{-1}$; (a) AC material with highlighted (yellow) extension twins indicated by arrows in its IPF map and (b) grain boundary misorientation distribution of as-cast material showing predominant tensile twin population around 86.3°, (c) HFG, (d) SFG, and (e) FFG [88].

superplastic elongation in Al alloys which was not present in the AZ91 Mg alloy. However, elongation of more than 600% and strain-rate sensitivity of more than 0.5 in FFG material confirmed that friction stir processed AZ91 behave superplastically at temperature of 350°C and strain rate of $5 \times 10^{-4} \, s^{-1}$ due to dynamic grain growth can be observed from the **Figure 11(e)**.

8. Conclusions

The effect of grain size on the superplastic deformation of metallic materials was studied. There were different combination of deformation mechanisms, accommodation mechanism, and rate-controlling mechanisms that governed the superplastic deformation which depends on the grain size, temperature, and strain rate. The following conclusions were obtained based on the detail study.

- The maximum elongation obtained by coarse-grained microstructure was between 500 and 800%. Solute-drag creep controlled by diffusion and GBS preceded by CDRV/CDRX was the deformation mechanisms in the coarse-grained microstructure.

- In fine-grained materials, GBS dominated the deformation mechanism. The accommodation mechanism could be either by "glide and climb" or by diffusion. If diffusion is the accommodation mechanism, it can be divided either by grain boundary diffusion or lattice diffusion which depends on the required activation energy.

- In UFG regime most of the materials exhibited either low-temperature superplasticity or high-strain-rate superplasticity. The mechanism in both cases is mostly observed to be GBS accommodated by dislocation slip.

- The kinetics of nano-grained deformation is different from that of their higher-scale grain sizes. The deformation mechanism in nano-grain structure is also GBS, but its accommodation by slip becomes difficult. The piled-up dislocations give rise to different accommodation mechanisms, namely, nano-twins, emission of Shockley partials, and stress-induced atomic shuffling.

- In materials with mixed grain size microstructure, the microstructure evolution during deformation needs to favor CDRX in the coarse-grained region in order to exhibit superior superplastic elongation—else finer-grained region controls the deformation.

Author details

Allavikutty Raja, Rengaswamy Jayaganthan*, Abhishek Tiwari
and Ch. Srinivasa Rakesh
Department of Engineering Design, Indian Institute of Technology Madras,
Chennai, India

*Address all correspondence to: edjay@iitm.ac.in

IntechOpen

References

[1] Backofen JRTWA, Avery DH. Superplasticity in Al-Zn alloy. Transactions of American Society for Metals. 1964;**57**:980

[2] Liu FC, Ma ZY. Superplasticity governed by effective grain size and its distribution in fine-grained aluminum alloys. Materials Science and Engineering A. 2011;**530**:548-558. DOI: 10.1016/j.msea.2011.10.018

[3] Edington JW, Melton KN, Cutler CP. Superplasticity. Progress in Materials Science. 1976;**21**:61-158

[4] Langdon TG. Grain boundary sliding revisited: Developments in sliding over four decades. Journal of Materials Science. 2006;**41**:597-609. DOI: 10.1007/s10853-006-6476-0

[5] Tan JC, Tan MJ. Superplasticity and grain boundary sliding characteristics in two stage deformation of Mg-3Al-1Zn alloy sheet. Materials Science and Engineering A. 2003;**339**:81-89

[6] Todd RI. Critical review of mechanism of superplastic deformation in fine grained metallic materials. Materials Science and Technology. 2000;**16**:1287-1294. DOI: 10.1179/026708300101507118

[7] Mukherjee AK. Superplasticity in Metals, ceramics and intermetallics, in: Plastic Deformation and Fracture of Materials. Wiley-VCH Verlag GmbH & Co. KGaA; 2003. pp. 407-460

[8] Yogesha KK, Joshi A, Raja A, Jayaganthan R. High-Cycle Fatigue Behaviour of Ultrafine Grained 5052 Al Alloy Processed Through Cryo-Forging. Cham: Springer; 2019. pp. 153-161. DOI: 10.1007/978-3-030-05728-2_14

[9] Logakannan KP, Verma R, Jayaganthan R, Velmurugan R. Effect of strain rate on tensile and fracture behavior of ultrafine grained Al6061 processed through cryorolling and warm rolling. Materials Today: Proceedings. 2018;**5**:17180-17187. DOI: 10.1016/J.MATPR.2018.04.127

[10] Verma R, Srinivasan A, Jayaganthan R, Nath SK, Goel S. Studies on tensile behaviour and microstructural evolution of UFG Mg-4Zn-4Gd alloy processed through hot rolling. Materials Science and Engineering A. 2017;**704**:412-426. DOI: 10.1016/J.MSEA.2017.08.032

[11] Laxmanappa SK, Jayaganthan R, Chakravarthy SR, Sarathi R. Size-dependent energetics and thermodynamic modeling of ZnO nanoparticles produced by electrical wire explosion technique. Materials Today: Proceedings. 2018;**5**:17293-17303. DOI: 10.1016/J.MATPR.2018.04.141

[12] Balakrishnan V, Roshan P, Goel S, Jayaganthan R, Singh IV. Experimental and XFEM simulation of tensile and fracture behavior of Al 6061 alloy processed by severe plastic deformation. Metallography, Microstructure, and Analysis. 2017;**6**:55-72. DOI: 10.1007/s13632-016-0332-7

[13] Fuloria D, Kumar N, Goel S, Jayaganthan R, Jha S, Srivastava D. Tensile properties and microstructural evolution of Zircaloy-4 processed through rolling at different temperatures. Materials and Design. 2016;**103**:40-51. DOI: 10.1016/J.MATDES.2016.04.052

[14] Mohammad H. Composition and microstructure effects on superplasticity in magnesium alloys. PhD thesis. 2010

[15] Kashyap BP, Arieli A, Mukherjee AK. Microstructural aspects of superplasticity. Journal of Materials Science. 1985;**20**:2661-2686. DOI: 10.1007/BF00553028

[16] del Valle JA, Ruano OA. Effect of annealing treatments on strain rate sensitivity and anisotropy in a magnesium alloy processed by severe rolling. Materials Science Forum. 2010;**638-642**:1524-1529. DOI: 10.4028/www.scientific.net/MSF.638-642.1524

[17] Doherty RD, Hughes DA, Humphreys FJ, Jonas JJ, Jensen DJ, Kassner ME, et al. Current issues in recrystallization: A review. Materials Science and Engineering A. 1997. DOI: 10.1016/S0921-5093(97)00424-3

[18] Knauer E, Freudenberger J, Marr T, Kauffmann A, Schultz L. Grain refinement and deformation mechanisms in room temperature severe plastic deformed Mg-AZ31. Metals. 2013;**3**:283-297. DOI: 10.3390/met3030283

[19] Jata KV, Semiatin SL. Continuous dynamic recrystallization during friction stir welding of high strength aluminum alloys. Scripta Materialia. 2000;**43**:743-749

[20] Huang K, Logé RE. A review of dynamic recrystallization phenomena in metallic materials. Materials and Design. 2016;**111**:548-574. DOI: 10.1016/j.matdes.2016.09.012

[21] Wadsworth J, Roberts CA, Rennhack EH. Creep behaviour of hot isostatically pressed niobium alloy powder compacts. Journal of Materials Science. 1982;**17**:2539-2546. DOI: 10.1007/BF00543885

[22] Morgan GC, Hammond C. Superplastic deformation properties of β-Ti alloys. Materials Science and Engineering. 1987;**86**:159-177. DOI: 10.1016/0025-5416(87)90450-2

[23] Lin D, Sun F. Superplasticity in a large-grained TiAl alloy. Intermetallics. 2004;**12**:875-883. DOI: 10.1016/J.INTERMET.2004.02.039

[24] Woo SS, Kim YR, Shin DH, Kim WJ. Effects of Mg concentration on the quasi-superplasticity of coarse-grained Al-Mg alloys. Scripta Materialia. 1997;**37**:1351-1358. DOI: 10.1016/S1359-6462(97)00275-3

[25] Taleff EM, Henshall GA, Nieh TG, Lesuer DR, Wadsworth J. Warmtemperature tensile ductility in Al-Mg alloys. Metallurgical and Materials Transactions A: Physical Metallurgy and Materials Science. 1998;**29**:1081-1091. DOI: 10.1007/s11661-998-1017-x

[26] Hosokawa H, Iwasaki H, Mori T, Mabuchi M, Tagata T, Higashi K. Effects of Si on deformation behavior and cavitation of coarse-grained Al-4.5Mg alloys exhibiting large elongation. Acta Materialia. 1999;**47**:1859-1867. DOI: 10.1016/S1359-6454(99)00047-6

[27] Chezan AR, De Hosson JTM. Superplastic behavior of coarse-grained aluminum alloys. Materials Science and Engineering A. 2005;**410-411**:120-123. DOI: 10.1016/J.MSEA.2005.08.118

[28] García-Bernal MA, Hernandez-Silva D, Sauce-Rangel V. Superplastic behavior of coarse-grained Al–Mg–Zn alloys. Journal of Materials Science. 2007;**42**:3958-3963. DOI: 10.1007/s10853-006-0368-1

[29] Ig Hong S. Influence of solute-dislocation interaction on the superplastic behavior and ductility of Al-Mg alloys. Scripta Materialia. 1999;**40**:217-222

[30] Kannan K, Johnson CH, Hamilton CH. A study of superplasticity in a modified 5083 Al-Mg-Mn Alloy. Metallurgical and Materials Transactions A. 1998;**29A**:1211-1998

[31] Diao H, Qayyume R, Wang T, Zhao S, Ma C. Superplastic behavior of coarse-grained Al-Mg alloy.

International Journal of Modern Physics: Conference Series. 2012;**6**:401-406. DOI: 10.1142/S2010194512003510

[32] Málek P. Superplasticity in a coarse-grained Zn-1.1 wt. % Al alloy. Czechoslovak Journal of Physics. 1988;**38**:406-408. DOI: 10.1007/BF01605414

[33] Lin D, Lin TL, Shan A, Li D. Superplasticity in Fe3Al-Ti alloy with large grains. Scripta Metallurgica et Materialia. 1994;**31**:1455-1460. DOI: 10.1016/0956-716X(94)90055-8

[34] Chu JP, Liu IM, Wu JH, Kai W, Wang JY, Inoue K. Superplastic deformation in coarse-grained Fe–27A1 alloys. Materials Science and Engineering A. 1998;**258**:236-242. DOI: 10.1016/S0921-5093(98)00939-3

[35] Mohri T, Mabuchi M, Nakamura M, Asahina T, Iwasaki H, Aizawa T, Higashi K. Microstructural evolution and superplasticity of rolled Mg-9Al-1Zn. Materials Science and Engineering A. 2000;**290**:139-144

[36] Lin K, Kang Z, Fang Q, Zhang J. Superplasticity at elevated temperature of a coarse-grained Mg-Li alloy. Advanced Engineering Materials. 2014;**16**:381-388. DOI: 10.1002/adem.201300302

[37] Wu X, Liu Y. Superplasticity of coarse-grained magnesium alloy. Scripta Materialia. 2002;**46**:269-274. DOI: 10.1016/S1359-6462(01)01234-9

[38] Zhou G, Chen L, Liu L, Liu H, Peng H, Zhong Y, et al. Low-temperature superplasticity and deformation mechanism of Ti-6Al-4V alloy. Materials. 2018;**11**:1212. DOI: 10.3390/ma11071212

[39] Rao MK, Mukherjee AK. Superplastic deformation behavior of a fine-grained aluminum alloy 7475. Materials Science and Engineering. 1986;**80**:181-193. DOI: 10.1016/0025-5416(86)90196-5

[40] Mikhaylovskaya AV, Yakovtseva OA, Sitkina MN, Kotov AD, Irzhak AV, Krymskiy SV, et al. Comparison between superplastic deformation mechanisms at primary and steady stages of the fine grain AA7475 aluminium alloy. Materials Science and Engineering A. 2018;**718**:277-286. DOI: 10.1016/J.MSEA.2018.01.102

[41] Fukuyo H, Tsal HC, Oyama T, Sherby OD. Super plasticity and Newtonian-viscous flow in fine-grained class I solid solution alloys. ISIJ Int. 1991;**31**:76-85

[42] Taleff EM, Ruano OA, Wolfenstine J, Sherby OD. Superplastic behavior of a fine-grained Mg–9Li material at low homologous temperature. Journal of Materials Research. 1992;**7**:2131-2135. DOI: 10.1557/JMR.1992.2131

[43] Kim WJ, Chung SW. Super-plasticity in fine-grained AZ61 magnesium alloy. Metallic Materials. 2000;**6**:255-259. DOI: 10.1007/BF03028220

[44] Wang YN, Huang JC. Texture characteristics and anisotropic superplasticity of AZ61 magnesium alloy. Materials Transactions. 2003;**44**:2276-2281

[45] Wang YN, Huang JC. Comparison of grain boundary sliding in fine grained Mg and Al alloys during superplastic deformation. Scripta Materialia. 2003;**48**:1117-1122. DOI: 10.1016/S1359-6462(02)00615-2

[46] Watanabe H, Mukai T, Higashi K. Deformation mechanism of fine-grained superplasticity in metallic materials expected from the phenomenological constitutive equation. Materials Transactions.

2004;**45**:2497-2502. DOI: 10.2320/ matertrans.45.2497

[47] Mikhaylovskaya AV, Yakovtseva OA, Golovin IS, Pozdniakov AV, Portnoy VK. Superplastic deformation mechanisms in fine-grained Al–Mg based alloys. Materials Science and Engineering A. 2015;**627**:31-41. DOI: 10.1016/J. MSEA.2014.12.099

[48] Xie C, Wang YN, Fang QH, Ma TF, Zhang AB, Peng WF, et al. Effects of cooperative grain boundary sliding and migration on the particle cracking of fine-grained magnesium alloys. Journal of Alloys and Compounds. 2017;**704**:641-648. DOI: 10.1016/j. jallcom.2017.02.057

[49] Wu MS, Nazarov AA, Zhou K. Misorientation dependence of the energy of symmetrical tilt boundaries in hcp metals: Prediction by the disclination-structural unit model. Philosophical Magazine. 2006;**84**:785-806. DOI: 10.1080/14786430310001646817

[50] Xu J, Guo B, Shan D. Severe plastic deformation techniques. In: Severe Plastic Deformation Technology. InTech; 2017. DOI: 10.5772/ intechopen.69503

[51] Kim WJ, Taleff E, Sherby OD. A proposed deformation mechanism for high strain-rate superplasticity. Scripta Metallurgica et Materialia. 1995;**32**:1625-1630. DOI: 10.1016/0956-716X(95)00246-R

[52] Nakahigashi J, Yoshimura H. Superplasticity and its application of ultra-fine grained Ti-6Al-4V alloy obtained through protium treatment. Metallurgical and Materials. 2002;**43**:2768-2772

[53] Neishi K, Horita Z, Langdon TG. Achieving superplasticity in ultrafine-grained copper: Influence of Zn and Zr additions. Materials Science and Engineering A. 2003;**352**:129-135. DOI: 10.1016/ S0921-5093(02)00868-7

[54] Ma ZY, Liu FC, Mishra RS. Superplastic deformation mechanism of an ultrafine-grained aluminum alloy produced by friction stir processing. Acta Materialia. 2010;**58**:4693-4704. DOI: 10.1016/J. ACTAMAT.2010.05.003

[55] Yuzbekova D, Mogucheva A, Kaibyshev R. Superplasticity of ultrafine-grained Al–Mg–Sc–Zr alloy. Materials Science and Engineering A. 2016;**675**:228-242. DOI: 10.1016/J. MSEA.2016.08.074

[56] Kawasaki M, Langdon T. Developing superplasticity in ultrafine-grained metals. Acta Physica Polonica A. 2015;**128**:470-478. DOI: 10.12693/ APhysPolA.128.470

[57] Langdon TG. Achieving superplasticity in ultrafine-grained metals. Mechanics of Materials. 2013;**67**:2-8. DOI: 10.1016/J. MECHMAT.2013.06.005

[58] Kawasaki M, Langdon TG. Evaluating the flow processes in ultrafine-grained materials at elevated temperatures. Materials Research. 2013;**16**:565-570

[59] Lee S, Horita ZJ. Superplasticity of ultra-fine grained 7075 alloy processed by high-pressure torsion. Materials Science Forum. 2014;**794-796**:807-810. DOI: 10.4028/www.scientific.net/ MSF.794-796.807

[60] Bobruk EV, Murashkin MY, Lomakin IV, Kazykhanov VU, Valiev RZ. Low temperature superplasticity of high-strength ultrafine-grained Al 7050 alloy. IOP Conference Series. Materials Science and Engineering. 2019;**461**:1-6. DOI: 10.1088/1757-899X/461/1/012090

[61] Edalati K, Masuda T, Arita M, Furui M, Sauvage X, Horita Z, et al. Room-temperature superplasticity in an ultrafine-grained magnesium alloy. Scientific Reports. 2017;**7**:2662. DOI: 10.1038/s41598-017-02846-2

[62] Kim D, Won JW, Park CH, Hong JK, Lee T, Lee CS. Enhancing superplasticity of ultrafine-grained Ti-6Al-4V without imposing severe plastic deformation. Advanced Engineering Materials. 2019;**21**:1-4. DOI: 10.1002/adem.201800115

[63] Mishra RS, McFadden SX, Mukherjee AK. Analysis of tensile superplasticity in nanomaterials. Materials Science Forum. 1999;**304-306**:31-38. DOI: 10.4028/www.scientific.net/MSF.304-306.31

[64] Ovid'ko IA. Superplasticity and ductility of superstrong nanomaterials. Reviews on Advanced Materials Science. 2005;**10**:89-104

[65] Warner DH, Sansoz F, Molinari JF. Atomistic based continuum investigation of plastic deformation in nanocrystalline copper. International Journal of Plasticity. 2006;**22**:754-774. DOI: 10.1016/J.IJPLAS.2005.04.014

[66] Sergueeva AV, Mara NA, Mukherjee AK. Grain boundary sliding in nanomaterials at elevated temperatures. Journal of Materials Science. 2007;**42**:1433-1438. DOI: 10.1007/s10853-006-0697-0

[67] Van Swygenhoven H, Derlet PM. Grain-boundary sliding in nanocrystalline fcc metals. Physical Review B. 2001;**64**:224105. DOI: 10.1103/PhysRevB.64.224105

[68] Seo JH, Yoo Y, Park NY, Yoon SW, Lee H, Han S, et al. Superplastic deformation of defect-free Au nanowires via coherent twin propagation. Nano Letters. 2011;**11**:3499-3502. DOI: 10.1021/nl2022306

[69] Ovid'ko IA, Skiba NV. Nanotwins induced by grain boundary deformation processes in nanomaterials. Scripta Materialia. 2014;**71**:33-36. DOI: 10.1016/J.SCRIPTAMAT.2013.09.028

[70] Valiev RZ, Islamgaliev RK, Semenova IP. Superplasticity in nanostructured materials: New challenges. Materials Science and Engineering A. 2007;**463**:2-7. DOI: 10.1016/J.MSEA.2006.08.121

[71] Alizadeh R, Mahmudi R, Ngan AHW, Huang Y, Langdon TG. Superplasticity of a nano-grained Mg-Gd-Y-Zr alloy processed by high-pressure torsion. Materials Science and Engineering A. 2016;**651**:786-794. DOI: 10.1016/j.msea.2015.10.094

[72] Edalati K, Horita Z, Valiev RZ. Transition from poor ductility to room-temperature superplasticity in a nanostructured aluminum alloy. Scientific Reports. 2018;**8**:6740. DOI: 10.1038/s41598-018-25140-1

[73] Mansoor B, Ghosh AK. Microstructure and tensile behavior of a friction stir processed magnesium alloy. Acta Materialia. 2012;**60**:5079-5088. DOI: 10.1016/j.actamat.2012.06.029

[74] Witkin D, Lee Z, Rodriguez R, Nutt S, Lavernia E. Al–Mg alloy engineered with bimodal grain size for high strength and increased ductility. Scripta Materialia. 2003;**49**:297-302. DOI: 10.1016/S1359-6462(03)00283-5

[75] Oskooie MS, Asgharzadeh H, Kim HS. Microstructure, plastic deformation and strengthening mechanisms of an Al-Mg-Si alloy with a bimodal grain structure. Journal of Alloys and Compounds. 2015;**632**:540-548. DOI: 10.1016/j.jallcom.2015.01.229

[76] Wang Y, Chen M, Zhou F, Ma E. High tensile ductility in a

nanostructured metal. Nature. 2002;**419**:912-914

[77] Cáceres CH, Selling BI. Casting defects and the tensile properties of an AlSiMg alloy. Materials Science and Engineering A. 1996;**220**:109-116. DOI: 10.1016/S0921-5093(96)10433-0

[78] Begum S, Chen DL, Xu S, Luo AA. Low cycle fatigue properties of an extruded AZ31 magnesium alloy. International Journal of Fatigue. 2009;**31**:726-735. DOI: 10.1016/J.IJFATIGUE.2008.03.009

[79] Perron A, Politano O, Vignal V. Grain size, stress and surface roughness. Surface and Interface Analysis. 2008;**40**:518-521. DOI: 10.1002/sia.2849

[80] Liu WC, Dong J, Zhang P, Korsunsky AM, Song X, Ding WJ. Improvement of fatigue properties by shot peening for Mg-10Gd-3Y alloys under different conditions. Materials Science and Engineering A. 2011;**528**:5935-5944. DOI: 10.1016/j.msea.2011.04.004

[81] Figueiredo RB, Sabbaghianrad S, Giwa A, Greer JR, Langdon TG. Evidence for exceptional low temperature ductility in polycrystalline magnesium processed by severe plastic deformation. Acta Materialia. 2017;**122**:322-331. DOI: 10.1016/j.actamat.2016.09.054

[82] Watanabe H, Tsutsui H, Mukai T, Kohzu M, Tanabe S, Higashi K. Deformation mechanism in a coarse-grained Mg±Al±Zn alloy at elevated temperatures. International Journal of Plasticity. 2001;**17**:387-397

[83] Fan W, Kashyap BP, Chaturvedi MC. Effect of layered microstructure and its evolution on superplastic behaviour of AA 8090 Al-Li alloy. Materials Science and Technology. 2001;**17**:439-445

[84] Pancholi V, Kashyap B. Effect of local strain distribution on concurrent microstructural evolution during superplastic deformation of Al–Li 8090 alloy. Materials Science and Engineering A. 2003;**351**:174-182. DOI: 10.1016/S0921-5093(02)00849-3

[85] Pradeep S, Pancholi V. Superplastic forming of multipass friction stir processed aluminum-magnesium alloy. Metallurgical and Materials Transactions A: Physical Metallurgy and Materials Science. 2014;**45**:6207-6216. DOI: 10.1007/s11661-014-2573-x

[86] Álvarez-Leal M, Orozco-Caballero A, Carreño F, Ruano OA. Superplasticity in a commercially extruded ZK30 magnesium alloy. Materials Science and Engineering A. 2018;**710**:240-244. DOI: 10.1016/J.MSEA.2017.10.093

[87] Pradeep S, Pancholi V. Effect of microstructural inhomogeneity on superplastic behaviour of multipass friction stir processed aluminium alloy. Materials Science and Engineering A. 2013;**561**:78-87

[88] Raja A, Biswas P, Pancholi V. Effect of layered microstructure on the superplasticity of friction stir processed AZ91 magnesium alloy. Materials Science and Engineering A. 2018;**725**:492-502. DOI: 10.1016/J.MSEA.2018.04.028

[89] Dunne FPE. Inhomoneneity of microstructure in superplasticity and its effect on ductility. International Journal of Plasticity. 1998;**14**:413-433

[90] Pancholi V, Raja A, Rohit K. Deformation Behavior of Inhomogeneous Layered Microstructure. 2017. DOI: 10.4028/www.scientific.net/MSF.879.1437

[91] Gourdet S, Montheillet F. A model of continuous dynamic recrystallization. Acta Materialia. 2003;**51**:2685-2699

[92] Hallberg H, Wallin M, Ristinmaa M. Modeling of continuous dynamic

recrystallization in commercial-purity aluminum. Materials Science and Engineering A. 2010;**527**:1126-1134. DOI: 10.1016/j.msea.2009.09.043

[93] Guo-Zheng Q. Characterization for dynamic recrystallization kinetics based on stress-strain curves. In: Wilson P, editor. Recent Developments in the Study of Recrystallization. London, UK: InTech; 2013. pp. 61-88. DOI: 10.5772/54285